Experimental Cell Research 365 (2018) 106–118

Contents lists available at ScienceDirect

Experimental Cell Research

journal homepage: www.elsevier.com/locate/yexcr

Lab-on-a-chip platforms for quantification of multicellular interactions in bone remodeling

Estee L. George*, Sharon L. Truesdell, Spencer L. York, Marnie M. Saunders

The University of Akron, Olson Research Center 319, 302 E. Buchtel Ave., Akron 44325-0302, OH, USA

ARTICLE INFO

Keywords:
Bone remodeling
Lab-on-a-chip
Mechanical load
Mechanotransduction
Microfluidic

ABSTRACT

Researchers have been using lab-on-a-chip systems to isolate factors for study, simulate laboratory analysis and model cellular, tissue and organ level processes. The technology is increasing rapidly, but the bone field has been slow to keep pace. Novel models are needed that have the power and flexibility to investigate the elegant and synchronous multicellular interactions that occur in normal bone turnover and in disease states in which remodeling is implicated. By removing temporal and spatial limitations and enabling quantification of functional outcomes, the platforms should provide unique environments that are more biomimetic than single cell type systems while minimizing complex systemic effects of in vivo models. This manuscript details the development and characterization of lab-on-a-chip platforms for stimulating osteocytes and quantifying bone remodeling. Our platforms provide the foundation for a model that can be used to investigate remodeling interactions as a whole or as a standard mechanotransduction tool by which isolated activity can be quantified as a function of load.

1. Introduction

In the past five years, important in vitro studies have been performed that contribute to our understanding of osteocyte mechanotransduction—the process by which osteocytes sense mechanical load and signal to other cells to orchestrate bone remodeling. Much of this work focuses on the effects of fluid flow on osteocyte secretory factors that influence osteogenesis and bone remodeling by osteoclasts (bone resorbing cells) and osteoblasts (bone forming cells). For example, Govey et al. performed transcriptomic and proteomic analyses following stimulation of osteocyte-like cells with oscillating fluid flow. Importantly, chemokines *Cxc11* and *Cxcl12*—which may act as paracrine signals for the recruitment of osteoclasts and osteoblasts—were shown to be responsive to fluid flow for the first time [13]. Additionally, Chen and coworkers showed fluid shear stress of osteocytes promotes osteogenic lineage commitment. After 24 h of mechanical stimulation, conditioned medium (CM) was added to mesenchymal progenitor cells. Following 24 h of exposure to the CM, DNA methylation decreased for osteogenic markers, and gene expression of later osteogenic markers increased [5]. Both of these studies provide valuable information that enhances our appreciation for osteocyte signaling during mechanotransduction.

Moreover, novel techniques that model the physiological environment during mechanotransduction and subsequent bone remodeling are being devised. X. Edward Guo's group from Columbia University has focused on the development of multiscale experimental systems for the study of mechanical stimulation and associated tissue adaptation. These platforms include an ex vivo murine tibia model for the study of osteocyte mechanosensation and early mechanotransduction. The model incorporates a mechanical loading apparatus that delivers cyclic compressive loads to the whole bone. In this way, tissue-level stimulation can be induced and the osteocytes' early response investigated within the native environment. Another of Guo's experimental systems is a trabecular bone explant model. Trabecular bone samples containing osteocytes and on which osteoblasts are cultured are maintained within a loadable perfusion bioreactor. Load is applied, osteocytes signal to osteoblasts, and histological and mechanical property changes are measured. A final technique developed by Guo and coworkers enables visualization of changes in osteocytes' cytoskeletal features during fluid flow. High temporal resolution and reconstruction of quasi-three-dimensional images facilitate characterization of the immediate mechanical activities of these cytoskeletal components [4]. These systems show great promise in moving forward our understanding of the complex mechanisms by which osteocytes function to direct bone turnover and adaptation. We hope to add to this body of work through use of a physiological lab-on-a-chip (LOC) that integrates multicellular interactions during bone remodeling.

Because miniature LOC platforms have the ability to incorporate multifunctional elements to construct complete analytic microsystems [7,19], they have proven applicable to research in the biological

* Corresponding author.
E-mail addresses: eg55@zips.uakron.edu (E.L. George), slt79@zips.uakron.edu (S.L. Truesdell), sly15@zips.uakron.edu (S.L. York), mms129@uakron.edu (M.M. Saunders).

https://doi.org/10.1016/j.yexcr.2018.02.027
Received 6 December 2017; Received in revised form 22 February 2018; Accepted 23 February 2018
Available online 28 February 2018
0014-4827/

sciences, including genomics, proteomics, clinical diagnostics and drug discovery [9,12,19]. LOCs house individual controlled environments that are unable to be replicated through other means–these have proven advantageous in cell culture [7,9,11]. For example, microfluidic devices are equipped to culture small numbers of cells under precisely regulated conditions with limited consumption of materials [7]. These benefits have been exploited, and substantial work aimed at developing systems to mimic tissues, organs and organ systems has been completed [7,9,11,12].

While many areas of research have adopted this technology to great benefit, the bone field has been slow to incorporate the advantages these systems provide. Presently, much of what is known about the response of bone cells to mechanical stimulation has been gathered from in vitro mechanotransduction studies in which cells are isolated as a single cell type in an artificial environment and in the absence of native milieu [3,6,14,15,18,29–31]. These systems are not able to adequately mimic the physiologic environment of the bone or integrate many of the fundamental elements known to be crucial in mechanotransduction [9]. An important exception is a microfluidic co-culture platform developed by Middleton et al. that allows for the study of osteocyte-osteoclast communication in the presence of shear stress. The device consists of three microchannels in parallel separated by high resistance side channels. The three main microchannels simultaneously house mechanically stimulated osteocyte-like cells, osteoclast precursors and unstimulated osteocyte-like cells, respectively, to promote signaling among populations. Experimentation with this physiological setup led to some interesting discoveries. For example, it was observed that osteoclast precursor density and osteoclastogenesis increase toward unstimulated osteocyte-like cells and that osteocyte mechanosensitivity increases when in co-culture with osteoclasts [23]. Given its physiological relevance, this work contributes markedly to our comprehension of osteocyte-osteoclast signaling during mechanostimulation.

Our goal is to develop a platform that minimally incorporates the three key types of bone cells–osteocytes, osteoblasts and osteoclasts–and removes temporal and spatial limitations. This system will enable investigation not possible with single cell in vitro or in vivo models. For example, bone cells possess vastly dissimilar lifespans; in fact, the lives of osteocytes and osteoclasts differ by years [21]. And, the duration of resorption is about three weeks, while the formation phase lasts approximately three months. Further, osteoblasts and osteoclasts are not observed in the same location simultaneously during the process of remodeling. A LOC can remove these restrictions and enable concurrent study of any combination of cell types. Finally, while mechanotransduction studies generally quantify biomarker activity that is *indicative* of function, the LOC platform can be designed to enable quantification of functional outcomes, i.e. bone formation and resorption. As such, LOC technology offers opportunities to bridge the gap between isolated in vitro experiments and animal models, providing complex information yet controlling for confounding factors found within in vivo systems [15].

2. Bone's multicellular interactions

To develop biomimetic bone systems, multicellular interactions involved in mechanically-induced bone remodeling should be incorporated (Fig. 1). In their quiescent state (Fig. 1a), networked osteocytes (blue) communicate via gap junctions (GJ, black) with nearby osteocytes and osteoblastic bone lining cells (yellow) on the bone surface. At the initiation of damage (Fig. 1b-c), fractures arise, impairing osteocytes and potentially severing their processes. Simultaneously, conformational changes in bone lining cells result in the exposure of the bone surface and the formation of a canopy between endothelial cells (light green) of the neighboring vasculature and the bone lining cells (Fig. 1d). As the vasculature is exposed to the bone surface, circulating hematopoietic cells escape and converge on the surface, forming multinucleated osteoclasts (purple) that resorb bone (Fig. 1e). Upon the removal of necrotic tissue (Fig. 1f), osteoblasts (dark green) are drawn to the surface to lay down osteoid, which eventually mineralizes (Fig. 1g). Some of the osteoblasts become encapsulated in the matrix and undergo morphological and functional changes to live out the rest of their existence as osteocytes. As the bone is replaced, communication networks are restored, and the canopy is dismantled as the quiescent bone lining cells (inactive osteoblasts) return to the bone surface. While this general process is known [8,27], there is still much to understand regarding the mechanisms and pathways involved in bone remodeling [24], most of which extends beyond the information obtainable from traditional in vitro systems. Development of a bone remodeling LOC provides the benefit of a flexible system that enables the study of these factors in isolation and in combination and is minimally as effective as current in vitro single cell type models.

3. LOC platforms for bone study

Osteocytes are mechanosensory cells uniquely positioned within the bone matrix to sense stimuli and, in turn, direct osteoblasts and osteoclasts in remodeling. While it is known that osteoblasts form bone and osteoclasts resorb bone, the coupling interactions have yet to be fully elucidated. Arguments have been made for soluble factors, direct contact and cell-matrix interactions [33]. Likely, as osteoclasts resorb, signals are sent to osteoblasts or their precursors to minimize bone formation or keep them at bay until they are needed. Whether these signals originate from the osteocyte, osteoclast or environment remains to be determined. However, the net effect of all co-factors should support resorption by suppressing concurrent formation. A similar case can be made for the formation phase. Because remodeling at a given site can take months to complete, there are many opportunities for such interactions; however, the bone field is only beginning to recognize the potential relevance of long-term interactions [34].

We have developed two LOC platforms to date. The first contains osteocytes cultured on polydimethylsiloxane (PDMS) that can be loaded by out-of-plane substrate distention. The second contains osteoclasts or osteoblasts cultured on appropriate substrates and enables quantification of bone resorption and formation. We seek to combine these devices into versatile LOC platform(s), like those shown in Fig. 2. The flexibility of platforms like these allows for the investigation of a multitude of remodeling interactions, pathways and paradigms. In Fig. 2a, the platform is designed to investigate osteoclast soluble activity on bone formation. In this configuration, osteoclasts are exposed to CM from mechanically stimulated osteocytes. The osteoblasts are, in turn, exposed to double CM which contains soluble signals from the osteoclasts in response to osteocyte stimulation. The effects of these soluble signals on bone formation are quantified. When compared to studies in which osteoblasts are exposed to CM from mechanically stimulated osteocytes or in which they are subjected to direct load, multicellular interaction effects (soluble activity) can begin to be understood. In Fig. 2b, contact interactions are incorporated by co-cultures of osteoclasts and osteoblasts. In this configuration, co-cultures are exposed to CM from mechanically stimulated osteocytes with bone resorption and formation measured. By comparing the results from the two configurations, one can systematically investigate the role of soluble signals compared to direct cell contact in mechanically induced bone remodeling. In addition, this platform can be used to explore contact-dependent cell-cell communication via gap junctional intercellular communication (GJIC). Given the availability of gap junction inhibitors (topical additives) and knock-down models, these configurations can be used to investigate GJIC-intact or GJIC–inhibited environments to determine the contribution of GJIC to cell contact synergy. In Fig. 2c, the platform is designed to challenge paradigms. Here, unstimulated osteocytes are exposed to CM from mechanically damaged (overloaded) osteocytes. After a period of time, co-cultures of osteoblasts and osteoclasts are exposed to this double CM and, again,

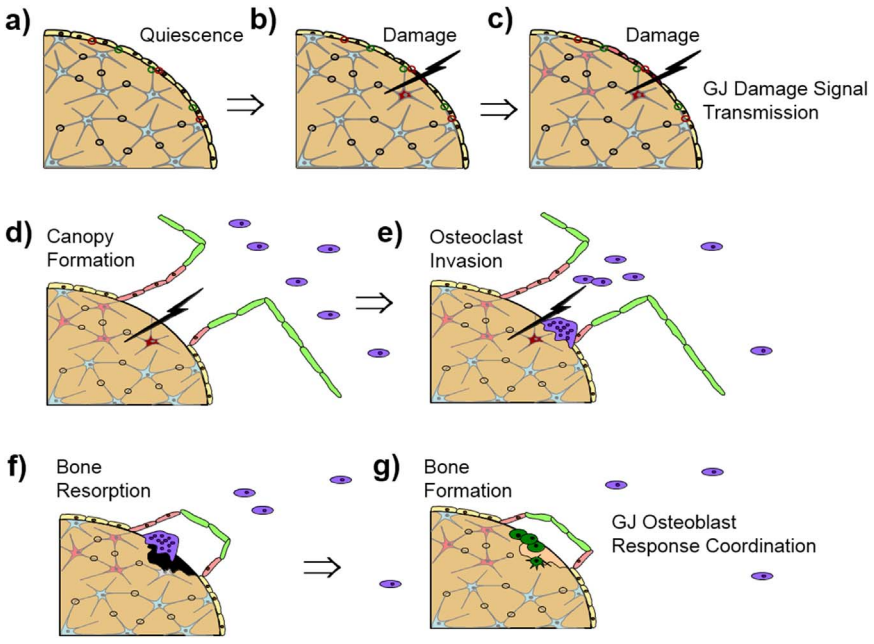

Fig. 1. Cartoon illustrating some of the key events that occur in bone remodeling. Inspired by ASBMR educational website video created by SM Ott. Illustration used here with permission. (Ott SM., 2008. Bone Growth and Remodeling. American Society for Bone and Mineral Research, Univ. of Washington, Seattle. http://depts.washington.edu/bonebio/ASBMRed/growth.html.).

bone resorption and formation are quantified. These experiments are designed to address the question: Is it the mechanically impaired osteocytes *or* the unstimulated osteocytes receiving soluble signals from the damaged osteocytes that are the more probable transducers of damage? The potency of damage signals can be assessed via quantification of functional activity.

4. Significance of LOCs

LOCs can be used to investigate bone-related events and diseases, such as fracture healing, distraction osteogenesis, bone tissue engineering, osteoporosis, bone metastasis, implant osteolysis and osteonecrosis of the jaw. For example, aspects of bisphosphonate-related osteonecrosis of the jaw (BRONJ) can be studied ideally using LOC platforms. In BRONJ, a bisphosphonate (BP) is administered as an antiresorptive drug to slow bone loss associated with diseases, such as osteoporosis and cancer metastasis. However, in some patients who have undergone tooth extractions, there is a drastic erosion of the jaw. Given that the etiology is poorly understood, LOCs can be used to model mechanical trauma (extraction) in the presence of a BP. Similar studies can be proposed to analyze interactions between bone cells and metastatic tumor cells in the early stages of metastatic progression. Once quantification studies are completed, the platform can be employed to investigate signaling pathways and disease mechanisms. In addition to research benefits, commercialization may lead to the development of a chip that can be used by pharmaceutical companies to test antiresorptive drug efficacy as well as investigate new drugs to measure unintended side effects on bone activity. While we do not suggest this approach will replace animal models, it may significantly diminish the number of drugs that proceed to animal studies as well as provide a model in which to study investigational new drug mechanisms of action, expediting time to market.

5. Materials and methods

5.1. Approach

We developed and characterized two LOCs: a mechanically loadable LOC which has been previously described and a functional activity LOC. Significant characterization work was completed to demonstrate our ability to fabricate a mechanically loadable device from PDMS using material property testing and parametric modeling [17,28,32,38–40,42]. This work illustrated that osteocytes directly contacting the collagen-coated PDMS within the LOC were not phenotypically altered on the polymer and that cell activity can be correlated to substrate location and strain [39]. Our initial goal is to investigate short-term exposure of osteocytes to overload and damage as well as its effects on bone remodeling. We have previously identified osteocyte loading ranges that are physiologic (≤10% substrate strain), physiologic/supraphysiologic (overload-inducing) and supraphysiologic (death-inducing) using mechanical testing, finite element analysis, digital image correlation techniques and quantification of osteocyte activity (e.g., viability) as a function of load. For example, we discovered lactate dehydrogenase (LDH)—a marker of cell viability—activity was significantly decreased following 15% (physiologic/supraphysiologic) loading [38,40,41]. In this manuscript, we demonstrate that the loadable platform can be used to study single cell type responses and is amenable to immunochemistry, imaging—fluorescence and scanning electron microscopy (SEM)—and protein analysis. We completed initial proof of concept by studying the effects of stimulated osteocytes on bone remodeling. We analyzed osteocytic factors and quantified the effects of CM on bone formation. Additionally, we performed studies to characterize osteoblasts and osteoclasts with the functional activity LOC and to verify they form bone on tissue culture (TC) treated polystyrene discs and resorb bone on wafer inserts within the device. Conclusively, we show feasibility and fidelity and demonstrate that our platforms facilitate mechanical load and bone remodeling.

5.2. Verification of osteocyte morphology and phenotype on PDMS in mechanically loadable LOC

MLO-Y4 osteocytes (a generous gift from Dr. Lynda Bonewald) were seeded at a density of 10^4 cells/cm^2 within T-25 culture flasks, maintained at 5% CO_2 and 37 °C and grown to 85–90% confluence in minimum essential alpha medium (MEMα, Gibco) supplemented with 5% calf serum, 5% fetal bovine serum (FBS, Hyclone) and 1% penicillin/streptomycin (Invitrogen). Cells were seeded at $2 * 10^4$ cells/cm^2 on PDMS wells coated with CTI (BD Bioscience) in 0.2 M acetic acid (Sigma) at a concentration of 5 μg/cm^2 for 1 h prior to rinsing in DPBS solution with calcium and magnesium (Hyclone). Osteocyte proliferation on PDMS was previously verified over 120 h and compared to proliferation on glass. LDH activity was verified at each time point (4,

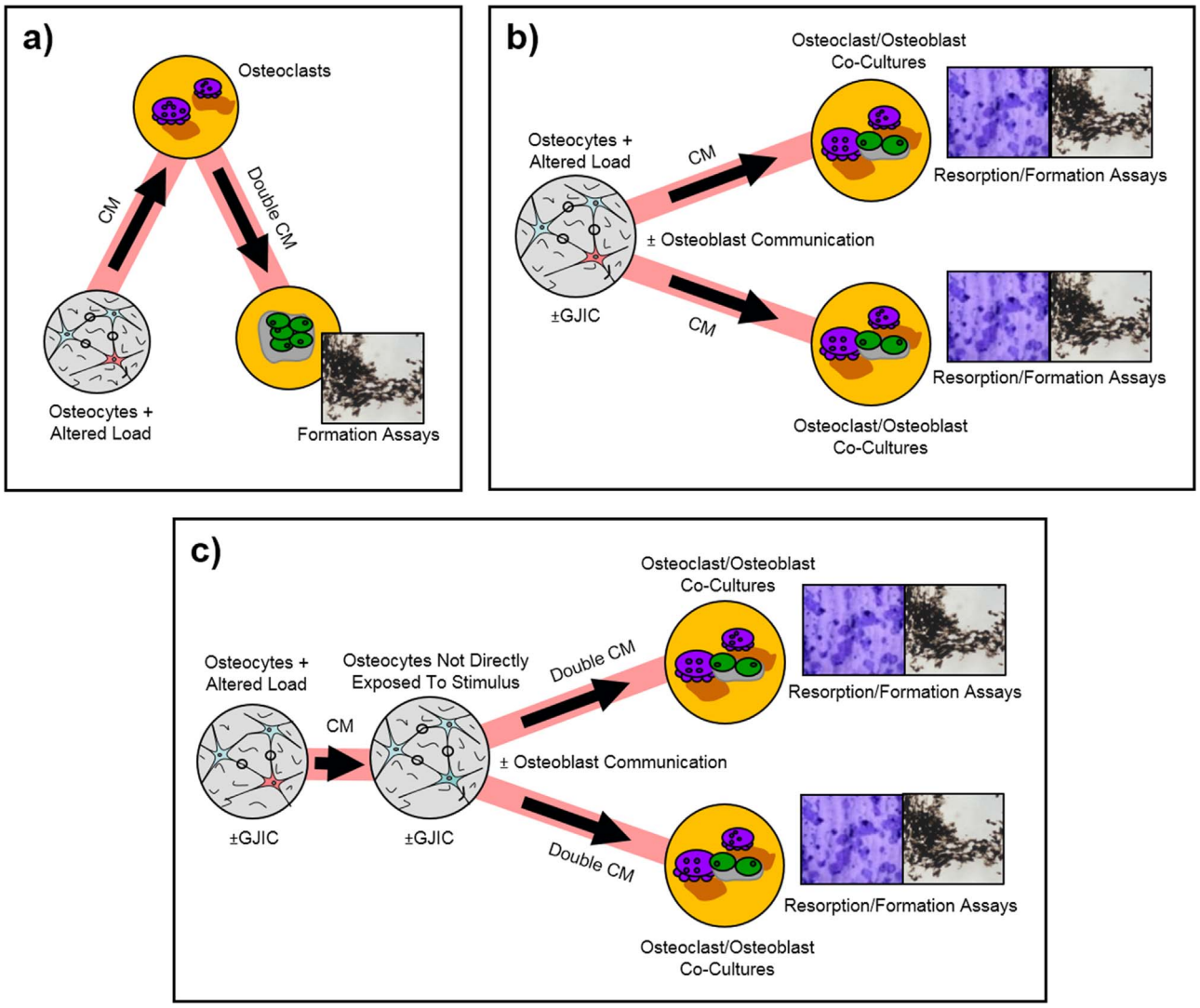

Fig. 2. Platform flexibility. In each LOC platform, osteocytes cultured on a collagen type I (CTI)-coated PDMS well are subjected to an altered load. In system (a), osteocyte CM is pumped from this well to a well containing osteoclasts cultured on a bone wafer. Osteoclasts respond to the soluble signals from the CM and generate signals of their own. Double CM is pumped from this well to a well containing osteoblasts cultured on a tissue culture (TC) treated polystyrene disc. Osteoblast bone formation in response to this double CM is quantified. In system (b), the direct effects of stimulated osteocyte CM on net bone resorption/formation are quantified. Again, osteocytes are subjected to an altered load, this time in either the presence or absence of GJIC. CM is pumped to two co-culture wells, one in which osteoblast communication is enabled and one in which it is inhibited. Bone resorption and formation are quantified. System (c) is employed similarly. This platform design is developed to study the relay of damage signals from stimulated (loaded, unloaded, etc.) osteocytes to unstimulated osteocytes. In this way, we can determine whether the directly stimulated osteocytes or those neighboring cells sensing damage signals carry most of the responsibility in mediating remodeling.

24, 48, 72, 96,120 h) [38]. Immunochemistry demonstrated the expression of key osteocyte markers, including dickkopf-1 (Dkk-1), receptor activator of nuclear factor kappa-B ligand (RANKL) and the gap junction protein Cx43 [40]. Briefly, cells on CTI-coated PDMS were washed in PBS, fixed using a paraformaldehyde solution at room temperature for 15 min and permeabilized for 10 min in a PBS solution containing 0.1% Triton X-100. Primary antibody was added in 1:50 or 1:100 ratios in 1% bovine serum albumin (BSA) solution and incubated overnight at 4 °C. Cells were washed in PBS, secondary antibody was added in a 1:500 ratio in 1% BSA solution and incubated at room temperature for 1 h. Cells were washed, mounted using PermaFluor™ mountant and coverslips and imaged. To visualize the actin cytoskeleton, rhodamine phalloidin with nuclear DAPI staining was completed. Following fixation in a 4% formaldehyde solution for 10 min, cells were rinsed in PBS and permeabilized in 0.2% Triton X-100 in PBS. Rhodamine phalloidin was added to the cells in a 2.5% v/v solution to 0.1% BSA in PBS. Following 20 min of incubation at room temperature, cells were washed in PBS. They were mounted using Vectashield with DAPI and imaged. SEM was also completed to verify morphology. For SEM, cells were fixed in a 2% glutaraldehyde, 2% paraformaldehyde solution in PBS for 15 min and washed with PBS and distilled water. Dehydration was performed over a period of 20 min; cells were dehydrated in 25% ethanol increments until immersed in 100% ethanol. Cells were critical point dried, sputter coated and imaged using SEM.

5.3. Use of mechanically loadable LOC

5.3.1. Mechanotransduction tool

To demonstrate the use of our loadable LOC as a mechanotransduction tool, osteocytes were maintained on CTI-coated PDMS wells within the device for a minimum of 96 h before loading. Cells were then exposed to 15 min of out-of-plane distention using a microactuated loading machine developed in-house and incubated for 90 min. Differential activity was then quantified. An alignment system was developed to enable precise manipulation of the LOC and cell tracking for correlating substrate strain with cellular activity. Based upon significant pilot characterization, physiologic loading (≤10% strain), physiologic/supraphysiologic loading (15–19% strain) and

supraphysiologic loading (19–34% strain) were generated by displacing the platen by 3804 μm, 5720 μm and 7240 μm, respectively [40]. Viability was quantified as a function of platen displacement with LDH staining and image analysis. CM was collected for cytokine quantification with ELISA or added to osteoblast cultures to quantify the effects of mechanical stimulation of osteocytes on bone formation.

As mentioned, LDH activity was completed to quantify cellular activity following loading. Osteocytes were washed with Hanks' Balanced Salt Solution (HBSS), then incubated in a reaction solution containing 5% Polypep (Sigma-Aldrich) base solution, 2 mM gly-gly (Sigma-Aldrich), 1.75 mg/ml nicotinamide adenine dinucleotide (NAD, Fluka), 60 mM lactic acid (Sigma-Aldrich), 3 mg/ml nitroblue tetrazolium (Sigma-Aldrich) and HBSS at a pH of 8.0. Following 1 h of incubation, cells were washed with distilled water and fixed in 4% paraformaldehyde overnight. Following fixation, cells were washed with distilled water and mounted with an aqueous mounting solution (VECTASHIELD®) and coverslips. Imaging and quantification followed.

ELISA panels (RayBiotech, Inc.) were used to analyze the concentration of soluble factors within CM after loading. Cytokine-specific antibodies were bound to a glass slide and incubated with the CM to be analyzed. To ensure specific detection, antibodies bound to biotin were added to the CM to form cytokine-antibody-biotin complexes after incubation. Streptavidin labeled with Cy3 was added in a third incubation. Cy3 was detected using a laser scanner and levels compared to standards, allowing the detection and quantification of cytokines. Sandwich ELISA panels were run three times in triplicate with medium collected and averaged, generating amean response across all runs.

5.3.2. Remodeling tool

To demonstrate the strength of the platform in quantifying the net result of bone's multicellular interactions, soluble effects of osteocyte loading on osteoblast bone formation were measured. In these experiments, CM generated following loading from physiologic (≤10% strain) or physiologic/supraphysiologic (15–19% strain) conditions were collected and used. During feedings, CM was introduced to osteoblast cultures as a 10% volume every three days in 50% volume replacements. All CM was generated in the osteocyte loading studies described above to verify initial consistency. Osteoblastic mineralization was assessed at day 26 using alizarin red staining and extraction, von Kossa staining and EDX. Following alizarin red staining, extraction was performed by adding 50 μl/cm^2 of 10% acetic acid to each well. Plates were placed on a benchtop shaker and incubated at room temperature overnight. Cells and stain were scraped from each well, pipetted into 1.5 ml tubes and heated at 85 °C for 10 min. Samples were then transferred to ice for 5 min and centrifuged at 18,000 × g on a tabletop microcentrifuge for 20 min. Finally, the supernatant from each sample was pipetted into a microplate in triplicate. Samples, standards and blanks were read at 405 nm using a microplate reader; absorbance values were converted to concentrations of alizarin red.

5.4. Design and fabrication of functional activity LOC

A mask was fabricated to accommodate three configurations of a functional activity LOC: a single well, a three-well linear arrangement and a three-well triangular arrangement (Fig. 3). The mask was designed in AutoCad and fabricated using Prototherm 12120 high-resolution stereolithography in a 0.05 mm build. A Plexiglass box with leveling screws in a tripod configuration was machined in-house to hold the mask (15.24 cm × 15.24 cm). PDMS was chosen as the material for the LOCs. A 10:1 elastomer base to curing agent (Sylgard 184, Dow Corning) ratio was used to make PDMS, which was vigorously mixed and desiccated. PDMS was poured into the mold and cured for 48 h at room temperature to make bases. Given the intended mechanical studies, well thicknesses of 0.5 mm were selected to avoid tearing the polymer upon loading [32]. TC treated polystyrene discs were inserted into the LOC wells that were to contain osteoblasts and adhered to the wells with uncured PDMS prior to sealing the chip with a PDMS lid. Bone wafers were inserted into the LOC wells that were to contain osteoclasts; they were also adhered to the wells with PDMS. PDMS sheets, or lids, ~4.0 mm thick were made as described above; access holes were bored through the lids using a biopsy punch 1 mm in diameter. The PDMS bases and lids were plasma oxidized for 30 s using a medium RF power setting (Plasma Cleaner, Harrick Plasma). One base and one lid per LOC were fused and baked at 65 °C for 10 min. Angled dispensing tips (18 Gauge, 0.5 in, 90°) were inserted into access holes within the lids, and epoxy stabilized the tips. They were then attached to silicone tubing (1/32″ ID). At the opposite end of each tube, an 18 Gauge needle and syringe were attached. The syringes were hooked up to a picopump (Pico Plus, Harvard Apparatus) for administration of liquids at 2 ml/h. Sterile liquids were pumped into the wells and channels of the devices. These included 70% ethanol, HBSS (for LOCs containing bone wafers) and distilled water. Osteoblasts were seeded using the picopump onto TC treated polystyrene discs and osteoclasts onto bone wafers within wells of the LOCs. All cells were maintained within LOCs at 5% CO_2 and 37 °C for appropriate lengths of time prior to analysis. Feedings were administered every 3 days by use of the picopump. While some cells grew within channels, this was curtailed by the geometry of the device. Channels were small enough so that cells preferred to stay within wells, where they could proliferate and spread appropriately. Additionally, movement of cells from wells into channels was decreased by use of the low flow rate—2 ml/h—during feedings. For analysis, PDMS lids were removed; as PDMS bonding is permanent, a scalpel was used to access wells. Osteocytes were analyzed directly in the wells, while discs and bone wafers were removed for osteoblast and osteoclast assays.

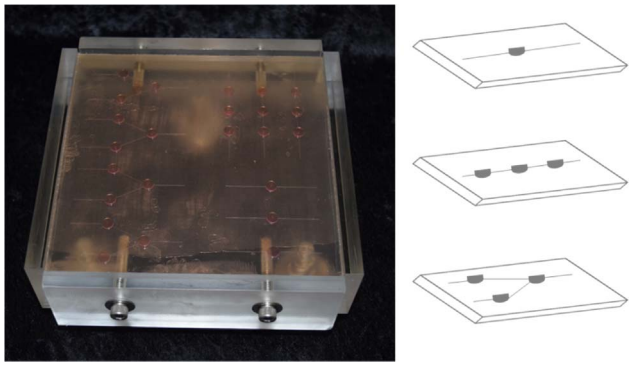

Fig. 3. Mask used in fabricating functional activity LOC. PDMS is poured onto the mask (left) and, upon curing, cut into chips containing different configurations of channels and wells (right).

5.5. Verification of osteoblast bone formation in functional activity LOC

Preliminary characterizations were performed in TC treated 96-well plates or polystyrene discs for confirmation of typical morphology, osteoblast differentiation and mineralization. MC3T3-E1 preosteoblasts (ATCC) were seeded at a density of 2500 cells/cm^2 and grown to 100% confluence in MEMα supplemented with 10% FBS and 1% penicillin/streptomycin. Cells were maintained at 5% CO_2 and 37 °C. Cells were induced to differentiate into osteoblasts at 100% confluence with a cocktail containing 50 μg/ml L-ascorbic acid and 10 mM β-glycerophosphate in culture medium. Cells were fed by 50% media replacements every 3 days for 26 days. To verify osteoblastic morphology, rhodamine phalloidin with DAPI staining was completed over the course of the culture period, and SEM was completed using methods previously described. At 26 days, bone formation was quantified with alizarin red and von Kossa staining. Elemental composition was determined by energy-dispersive X-ray spectroscopy (EDX). For alizarin red staining, cells were formalin fixed, stained with alizarin red dye solution for 30 min, washed and imaged. Percent area covered by bone

formation was determined using NIH ImageJ. Additionally, concentration of alizarin red dye extracted was performed by adding 10% acetic acid to culture wells and incubating overnight at room temperature. Cells were scraped and heated at 85 °C for 10 min prior to centrifugation. Absorbance was measured at 405 nm using a microplate and a standards range of 15.7 μM to 2 mM. For von Kossa staining, cells were fixed in 4% paraformaldehyde in PBS. A 5% silver nitrate solution was added, and cells were exposed to UV light for up to 60 min. Imaging followed, and percent area covered by bone formation was determined using ImageJ. For SEM/EDX, cells were fixed in a 2% glutaraldehyde, 2% paraformaldehyde solution in PBS for 15 min and washed with PBS and distilled water. Dehydration was performed over a period of 20 min; cells were dehydrated in 25% ethanol increments until immersed in 100% ethanol. Cells were critical point dried, sputter coated and imaged using SEM. EDX was performed in conjunction with SEM using Genesis software, EDAX. Sputter coating was not performed on EDX samples. Within LOCs, MC3T3-E1 preosteoblasts were seeded onto TC treated polystyrene discs (~5.4 mm ϕ) at a higher density of 10,000 cells/cm^2 to account for loss of cells within silicone tubing. Cells were cultured as described above. Cells were induced to differentiate and fed every 3 days by 100% media replacements for 49 days. Bone formation was verified by alizarin red and von Kossa staining as described above and quantified with ImageJ.

5.6. Verification of osteoclast bone resorption in functional activity LOC

Preliminary characterizations were performed on TC treated polystyrene or bovine bone wafers in 96-well plates for confirmation of typical osteoclast morphology, osteoclast formation and bone resorption. RAW 264.7 preosteoclasts (ATCC) were seeded onto TC treated polystyrene or bone wafers (~6 mm ϕ) at a density of 1000 cells/well in Dulbecco's modified eagle medium supplemented with 10% FBS and 1% penicillin/streptomycin. Cells were maintained at 5% CO_2 and 37 °C. Cells were induced to differentiate into osteoclasts at 24 h with a cocktail containing 120 ng/ml RANKL (R&D Systems) in culture medium. Cells were fed by 50% induction medium replacements every 2 days for 4, 5, 10 or 20 days. To verify cell fusion, typical morphology and tartrate-resistant acid phosphatase (TRAP) expression of cells cultured on polystyrene, TRAP stains and activity assays were performed at days 4, 5 and 10. Cells were fixed in 10% neutral buffered formalin and incubated in a solution of 50% methanol and 50% acetone for 3 min at room temperature. TRAP activity substrate (solution of sodium acetate, sodium tartrate and *para*-nitrophenylphosphate) was added, and cells were incubated at 5% CO_2 and 37 °C for 1 h. Following incubation, 100 μl of TRAP activity substrate from each sample were mixed with 50 μl 1 M NaOH, and microplate readings were taken at 405 nm. For TRAP staining, a commercially-available kit, 387A (Sigma Aldrich), was used. Cells were stained in a solution containing sodium nitrite, fast garnet, napthol and tartrate and imaged. Bone resorption was quantified with wafer pit staining at 20 days. Osteoclasts were removed from the wafers by 30 min of sonication and gentle cleaning with a cotton swab. The wafers were submerged in a toluidine blue solution for 2 min and rinsed briefly with distilled water. Imaging and determination of wafer area covered by resorption followed; quantification was performed by use of ImageJ. SEM verified that wafer regions stained with toluidine blue indicated functional resorption. Within LOCs, RAW 264.7 preosteoclasts were seeded onto bone wafers at higher densities—1500 cells/well and 56,000 cells/well—to account for loss of cells within silicone tubing. They were cultured and induced to undergo osteoclastogenesis as described above and fed by 100% induction medium replacements every 3 days. Given results of preliminary work (not shown) indicating that cells within LOCs take 50% longer to resorb efficiently, osteoclasts were cultured for 30 days in chips. Bone resorption was verified by toluidine blue staining and quantified with ImageJ. A timeline summarizing cell culture of osteoclasts and osteoblasts with control and LOC conditions is given in Fig. 4.

5.7. Statistics

For characterizations and experiments, D'agostino and Pearson tests were run to determine normality. Raw data were summarized by means with standard errors of the means. Analysis of continuous data was completed with ANOVA (parametric) or Mann Whitney U (nonparametric) techniques. Post-hoc comparisons of specific groups were made using the Tukey (parametric) or Bonferroni (nonparametric) methods. All analyses were completed with Instat (GraphPad). Characterizations and experiments were conducted a minimum of three times in triplicate, except for osteocyte CM studies on osteoblast bone formation given limited CM.

6. Results

6.1. Verification of osteocyte morphology and phenotype on PDMS in mechanically loadable LOC

Given that little work has been completed quantifying the effects of PDMS on osteocyte function, we completed comprehensive characterization studies. We have previously demonstrated that growth and proliferation on CTI-coated PDMS is not significantly different from that on CTI-coated glass [38]. As shown in Fig. 5, MLO-Y4 osteocytes on CTI-coated PDMS display the anticipated dendritic morphology. Rhodamine phalloidin and DAPI stains (Fig. 5a) reveal extensive cytoskeletal arrangement of actin filaments, and SEM imaging (Fig. 5b) shows that, by 72 h in culture, characteristic osteocyte morphology is observed. This correlates with the observation that coating and time in culture are required for MLO-Y4 cells to take on the osteocyte morphology. We have found this consistently occurs by 72 h; thus, osteocytes are plated a minimum of 72 h prior to experimentation. Immunocytochemistry (Fig. 5c) further corroborates the presence of known proteins critical to osteocyte function, including Dkk-1, RANKL and Cx43.

6.2. Use of mechanically loadable LOC

6.2.1. Mechanotransduction tool

Mechanotransduction studies employed a loading device and cell tracking system. A sketch of the loading platform fabricated in-house is shown in Fig. 6a and has been previously described and characterized [39]. Briefly, the microactuator raises a plunger that applies out-of-plane distention to the PDMS well (shown here with a single-well chip). A tracking system was developed and validated and enables cell strains (substrate strains) to be quantified as functions of grid location and actuator displacement (data not shown). To track positional reference, an alphanumeric grid was incorporated into the osteocyte PDMS well. Following characterization, actuator displacements generating physiologic (≤10% strain), physiologic/suparphysiologic (15–19% strain) and supraphysiologic (19–34% strain) loads were determined and used for all subsequent studies [40].

For viability assessment, LDH was quantified in osteocytes subjected to 15 min of physiologic, physiologic/supraphysiologic or supraphysiologic loading in intact and inhibited GJIC environments. As shown in Fig. 6b, 15 min of physiologic/supraphysiologic loading decreased cell activity by 14% over physiologic stimulation, and 15 min of supraphysiologic loading decreased cell activity by 21% over physiologic stimulation. Interpreting the supraphysiologic loading as essentially inductive to death, further work with this load was not pursued. Results demonstrate that the platform can be used to quantify the behavior of a single cell type as a function of load, not unlike standard mechanotransduction models. Further, they reinforce the importance of a role for GJIC in the osteocytes' response to mechanical loading, and they illustrate that short-term loading can be effectively administered in the chip.

Using ELISA cytokine panels, we identified over 40 cytokines that

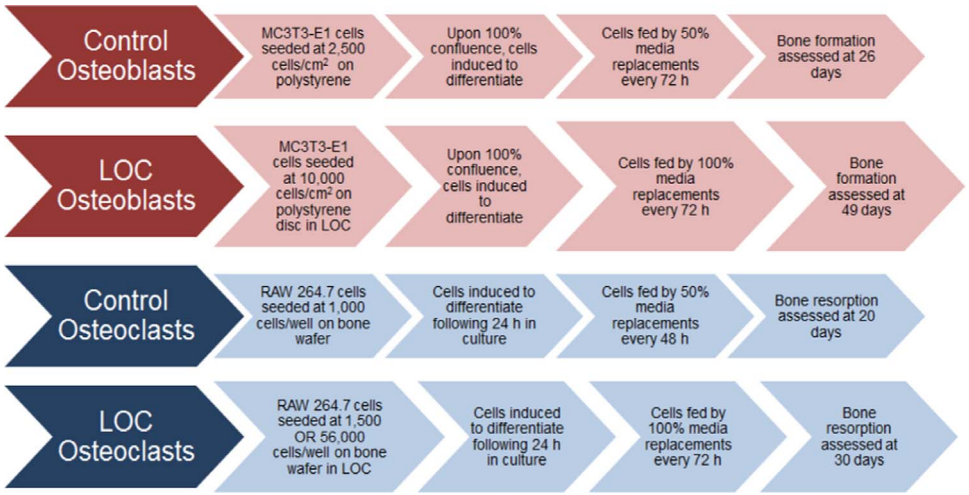

Fig. 4. Cell culture timeline providing seeding densities, substrates, differentiation inductions, feedings and functional activity assessments for control and LOC conditions.

were altered under short-term osteocyte loading. Although not an exhaustive list, several of the factors are identified in Fig. 6c, and some offer novel targets for further study. As shown in the color map, green colors indicate a percent increase, and red colors represent a percent decrease over unloaded controls. Percent changes were calculated from three readings, each of which was pooled from three identical treatment wells. Neural cell adhesion molecule 1 (NCAM-1), secreted frizzled related protein 3 (SFRP-3), decorin, ciliary neurotrophic factor (CNTF), serum amyloid A (SAA) and interleukin 1-receptor 3 (IL-1r3) were elevated by short-term physiologic loading. These findings were consistent with observations in previous studies. For example, NCAM-1 potentially curtails bone matrix formation, while SFRP-3 is a negative regulator of Wnt, and CNTF regulates trabecular and cortical bone in a sex-dependent manner [1,10,16]. Decorin is known to modulate collagen fibril formation, and SAA inhibits RANKL-induced osteoclast formation [2,25]. Cytokine decrease under physiologic load was observed with macrophage migratory inhibiting factor (MIF) and extracellular matrix metalloproteinase inducer (EMMPRIN). MIF is associated with bone loss in osteoporotic women, and EMMPRIN has been proposed to be involved in collagen breakdown and bone resorption [20,35]. The identification of remodeling-related cytokines is consistent with our findings that short-term physiologic stimulation increased bone formation, while physiologic/supraphysiologic stimulation associated with damage reduced formation. These cytokines offer many opportunities for further study using the LOC.

6.2.2. *Remodeling tool*

Preliminary quantification of bone formation as a function of osteocyte loading was completed using the remaining CM from the experiments summarized in Fig. 6. Studies were completed on confluent

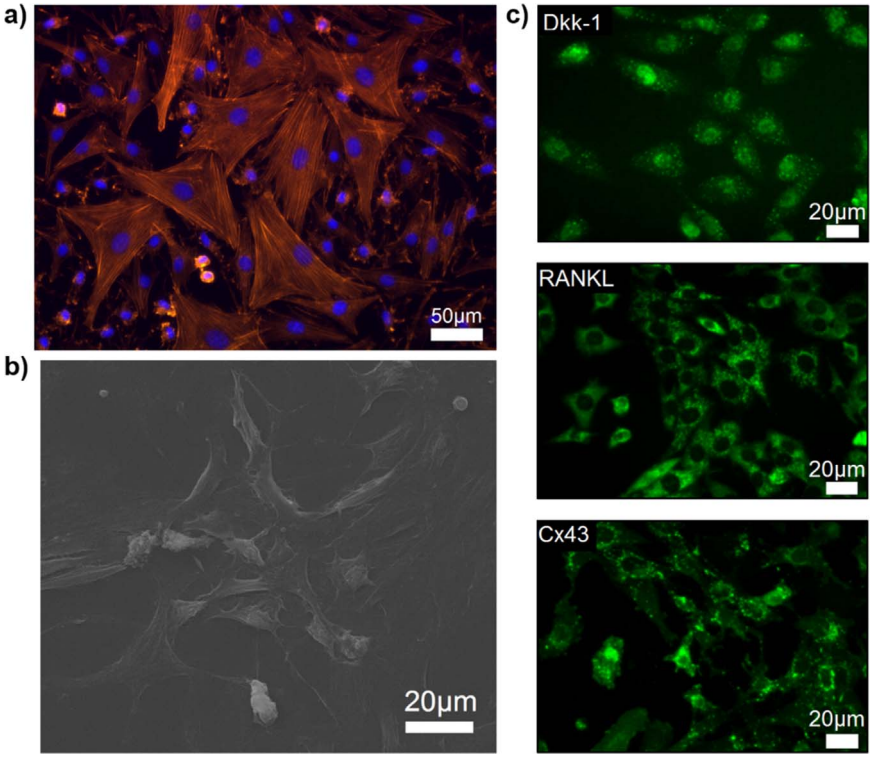

Fig. 5. Osteocyte characterization. a) Rhodamine phalloidin staining of MLO-Y4 osteocytes. b) SEM image showing typical MLO-Y4 osteocytes with dendritic processes. c) Immunocytochemistry staining of osteocyte proteins, Dkk-1, RANKL and the gap junction protein, Cx43.

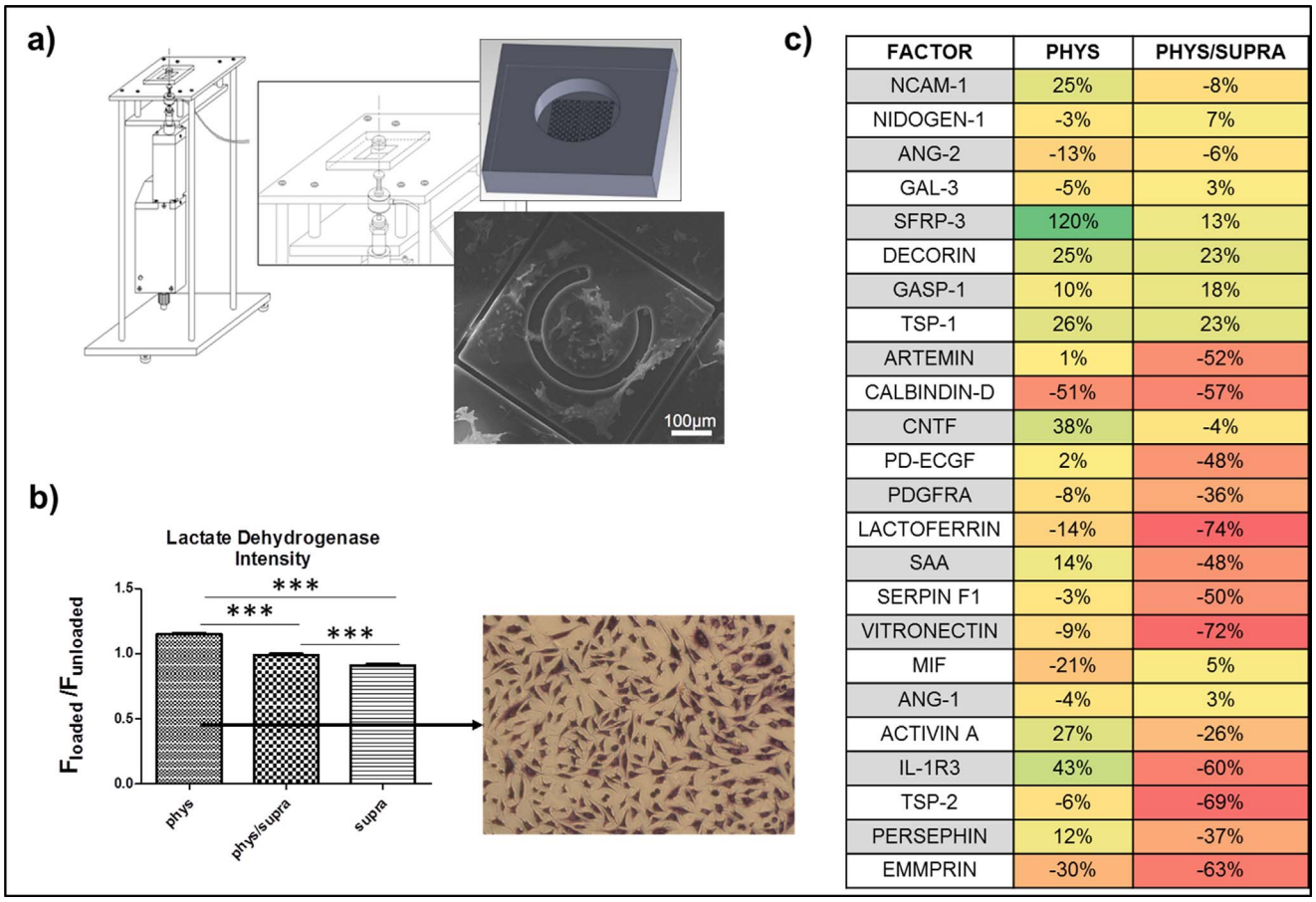

c)

FACTOR	PHYS	PHYS/SUPRA
NCAM-1	25%	-8%
NIDOGEN-1	-3%	7%
ANG-2	-13%	-6%
GAL-3	-5%	3%
SFRP-3	120%	13%
DECORIN	25%	23%
GASP-1	10%	18%
TSP-1	26%	23%
ARTEMIN	1%	-52%
CALBINDIN-D	-51%	-57%
CNTF	38%	-4%
PD-ECGF	2%	-48%
PDGFRA	-8%	-36%
LACTOFERRIN	-14%	-74%
SAA	14%	-48%
SERPIN F1	-3%	-50%
VITRONECTIN	-9%	-72%
MIF	-21%	5%
ANG-1	-4%	3%
ACTIVIN A	27%	-26%
IL-1R3	43%	-60%
TSP-2	-6%	-69%
PERSEPHIN	12%	-37%
EMMPRIN	-30%	-63%

Fig. 6. Development of microloading platform and osteocyte stimulation. a) Microloading platform developed in house for mechanical tenting of osteocytes to reproducible strain levels, PDMS well design with tracking grid and SEM of osteocytes seeded on PDMS well with tracking grid. b) LDH quantification of cell activity as a function of load type (top). A physiologic load induced significantly greater LDH activity than did physiologic/supraphysiologic or supraphysiologic loads. A physiologic/supraphysiologic load induced significantly greater LDH activity than did a supraphysiologic load. Scale bars represent standard errors of the means. c) CM cytokine activity showing expression (relative to unloaded controls) of biomarkers related to remodeling. Several apoptosis-related markers were also identified for further study. Values represent means of three samples in triplicate.

osteoblasts induced to differentiate; alizarin red and von Kossa stains are presented in Fig. 7a. In comparison to physiologically/supraphysiologically stimulated osteocytes, CM from physiologically stimulated osteocytes resulted in an increase in bone formation of 18% as indicated by alizarin red stain (Fig. 7b), 21% as indicated by von Kossa stain (Fig. 7c) and 36% as indicated by alizarin red extraction (Fid. 7d) (mean 25%). Given a small sample size (n = 3 or 6), rigorous statistics were not completed. Consistent with our independent classification of loading effects on osteocyte activity, however, physiologic loads that increased osteocyte activity had the expected effects of increasing osteoblast activity and bone formation. Similarly, physiologic/supraphysiologic loads that decreased osteocyte activity and incorporated overload as determined by LDH staining had the effects of decreasing osteoblast activity and bone formation.

6.3. Design and fabrication of functional activity LOC

The mask, Plexiglass box and PDMS platform used in fabrication of the functional activity LOC are illustrated in Fig. 8. The mask contained three different well configurations (Fig. 8a). The box (Fig. 8b) was equipped with leveling screws in a tripod configuration to ensure the mask remained level at all times and that a uniform well thickness of 0.5 mm was reproducible. The PDMS platform is shown with channel-connected wells prior to the addition of cells. Wells are 6 mm in diameter to accommodate commercial substrates. Channel widths and heights are 300 μm and 400 μm, respectively (Fig. 8c-d). Fig. 8e depicts MLO-Y4 osteocytes cultured in the LOC at 72 h. in Fig. 8f, a LOC containing cell culture medium is shown to demonstrate adequate filling. Evaporation studies (not shown) revealed that daily evaporation did not exceed 3%. Therefore, evaporation is not a concern given feedings will occur every 3 days.

6.4. Verification of osteoblast bone formation in functional activity LOC

MC3T3-E1 cells induced to differentiate formed bone on TC treated plates and polystyrene discs as well as on polystyrene discs within LOCs. Except with regard to the 16-day time point, concentrations of alizarin red extracted from TC treated plates at each time point (days 1, 2, 4 and 8 post-induction) were significant compared to the concentration at day 26 (2826 μM). Rhodamine phalloidin and DAPI staining (Fig. 9a) show confluent monolayers as well as typical osteoblast proliferation and morphology on plates at days 1, 2 and 16. SEM imaging (Fig. 9b) further confirms expected morphology and monolayer formation. Mineralization in LOCs (Fig. 9c) at day 49 is indicated by alizarin red, which stains calcium (top), and von Kossa, which stains phosphate (bottom). A direct comparison of surface area covered (Fig. 9d) revealed there was no significant difference in areas covered by calcium and phosphate (p-value: 0.1186). Percentages averaged 10.72% and 6.43%, respectively. EDX (Fig. 9e) revealed that nodule formation on TC treated polystyrene discs contained the expected Ca/P ratio of 1.7, indicating a strong correlation to native bone content [37]. No bone formation was observed in any of the non-induced cultures.

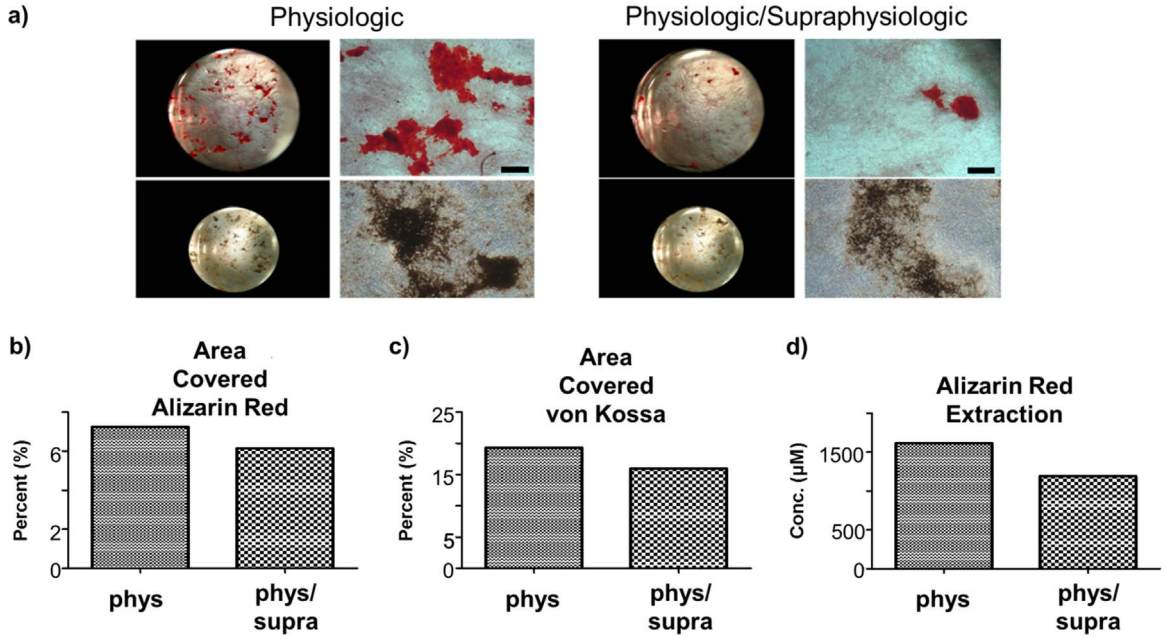

Fig. 7. Bone formation as a function of osteocyte loading. a) CM from physiologic loading induced increased bone formation (left) by osteoblastic cells in comparison to CM from physiologic/supraphysiologic loading (right). Alizarin red and von Kossa stains were performed for each plate corresponding to both loading conditions. Scale bars on the alizarin red (top) and von Kossa (bottom) images measure 500 μm and 200 μm, respectively. b, c,d) For physiologic studies, alizarin red extraction showed a 36% increase in dye concentration compared to physiologic/supraphysiologic studies, and percent area increases were 18% as indicated by alizarin red stains and 21% as indicated by von Kossa stains. Here, a sample size of at least 3 is represented.

6.5. Verification of osteoclast bone resorption in functional activity LOC

As shown in Fig. 10, RAW 264.7 cells undergo osteoclastogenesis by 4 days post-induction (Fig. 10a). TRAP activity was decreased by 46% between days 4 and 5 and by 63% between days 4 and 10. Therefore, it was determined that TRAP production was optimal at day 4 (Fig. 10c). SEM verified formation of resorption pits on bone wafers by 20 days in TC treated plates (Fig. 10b). Quantification of bone resorption via pit staining with toluidine blue was completed following 20 days of culture within plates and following 30 days of culture within LOCs (Fig. 10d). The percentages of area resorbed by osteoclasts seeded within LOCs at 1500 cells/well and at 56,000 cells/well after 30 days were not significantly different from the percentage of area resorbed by osteoclasts seeded at 1000 cells/well after 20 days.

7. Discussion

We advocate for the development of LOC bone remodeling platforms. These systems have the potential to systematically elucidate complex multicellular interactions in highly controlled and reproducible environments. As a proof of concept, we developed LOC platforms and verified that osteocytes, osteoblasts and osteoclasts were not functionally altered. Specifically, we demonstrated that osteoblasts form bone and osteoclasts resorb bone reproducibly in our model. We

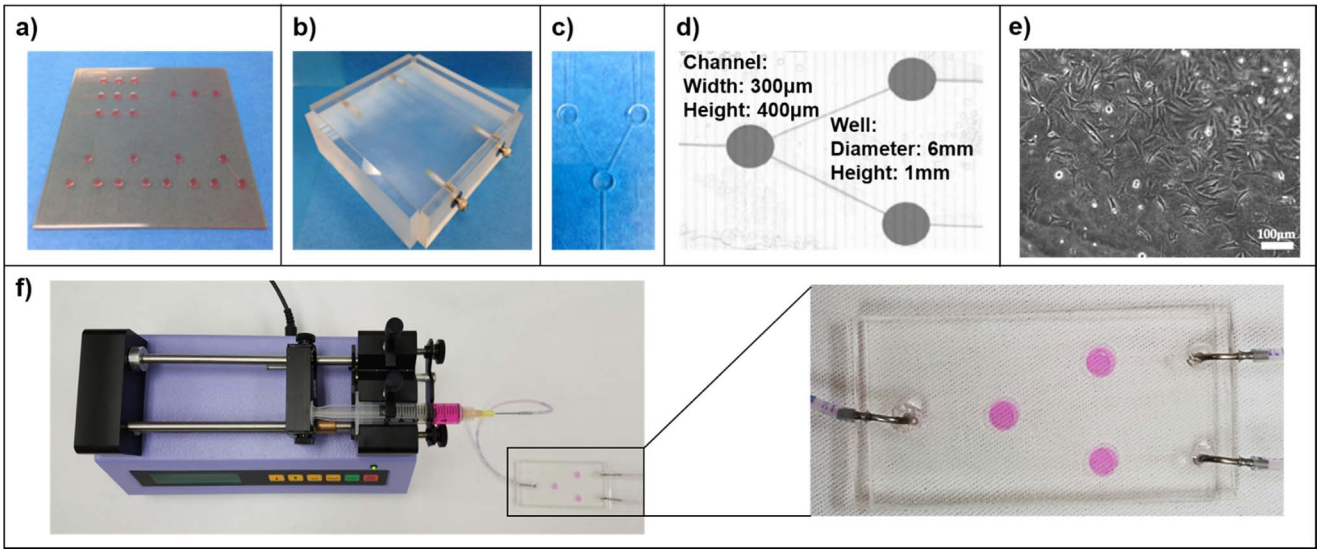

Fig. 8. Development of the LOC. LOC platforms are fabricated using a Prototherm 12120 mask (a) and pouring PDMS onto the mask placed in a Plexiglass box (b). The box enables well thicknesses to be adjusted and contains leveling screws in a tripod configuration to maintain alignment. The finished LOC houses channels 300 μm wide and 400 μm in height and wells 6 mm in diameter and 1 mm in height. (c, d). MLO-Y4 osteocytes are imaged within the LOC after 72 h in culture (e). Using a syringe, a picopump administers cell culture medium to microchannels and wells of a chip (f).

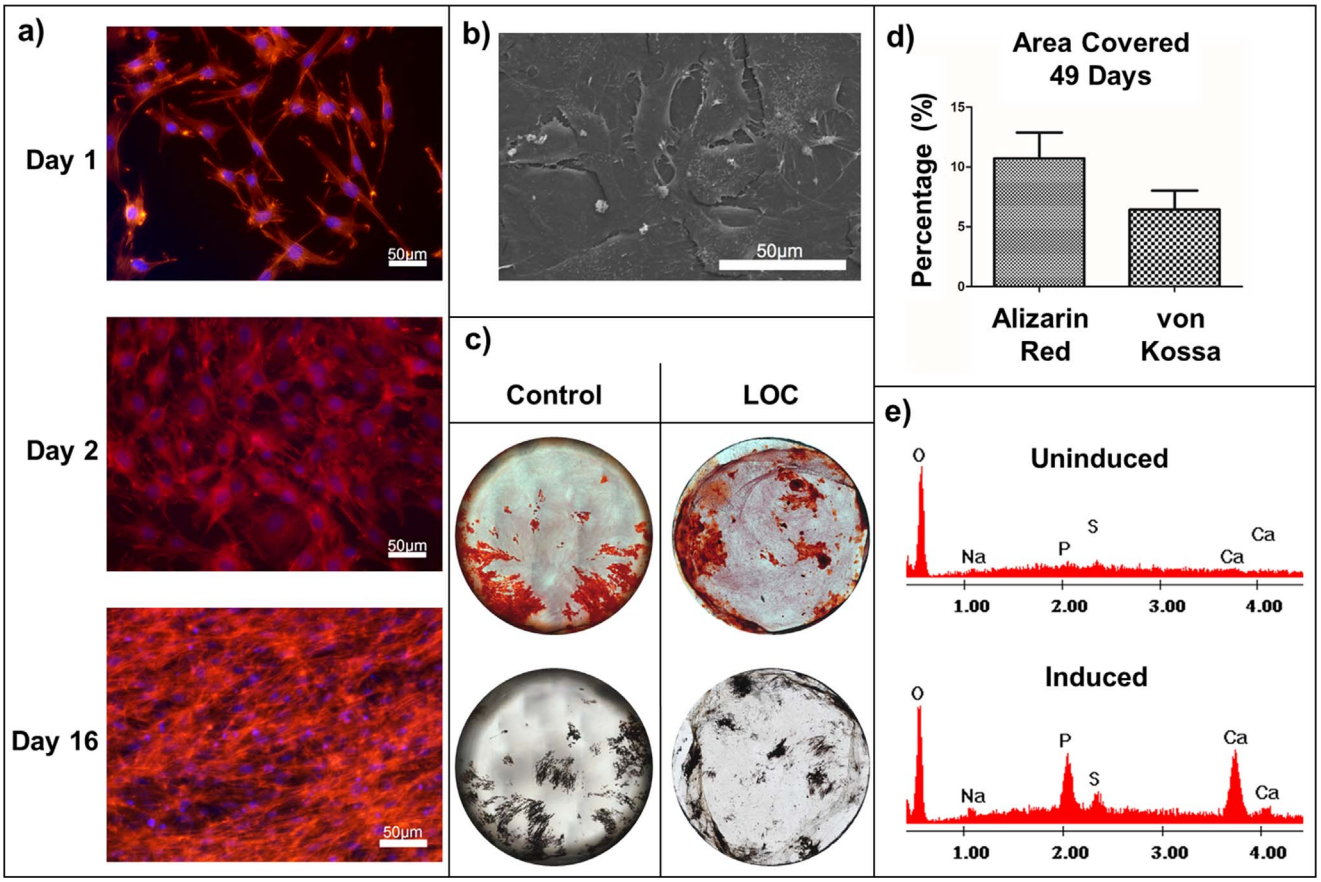

Fig. 9. Osteoblast Characterization. a) Rhodamine phalloidin images showing typical MC3T3-E1 cells in culture at days 1, 2 and 16 post-induction. b) SEM showing typical MC3T3-E1 cells in culture. c) TC treated wells at 26 days (left) and polystyrene discs from LOC at 49 days (right) post-induction and stained with alizarin red (top) and von Kossa (bottom). Discs measure approximately 5.4 mm in diameter. d) Percentages of disc area covered by alizarin red and von Kossa stains. Error bars represent standard errors of the means. e) Typical EDX of osteoblastic bone nodules in plates at 26 days from uninduced controls (top) and induced MC3T3-E1 cells (bottom), establishing baseline composition. Induced samples showed a 12-fold increase in calcium (Ca) and a 7-fold increase in phosphorous (P) over uninduced samples (Ca/P = 1.7).

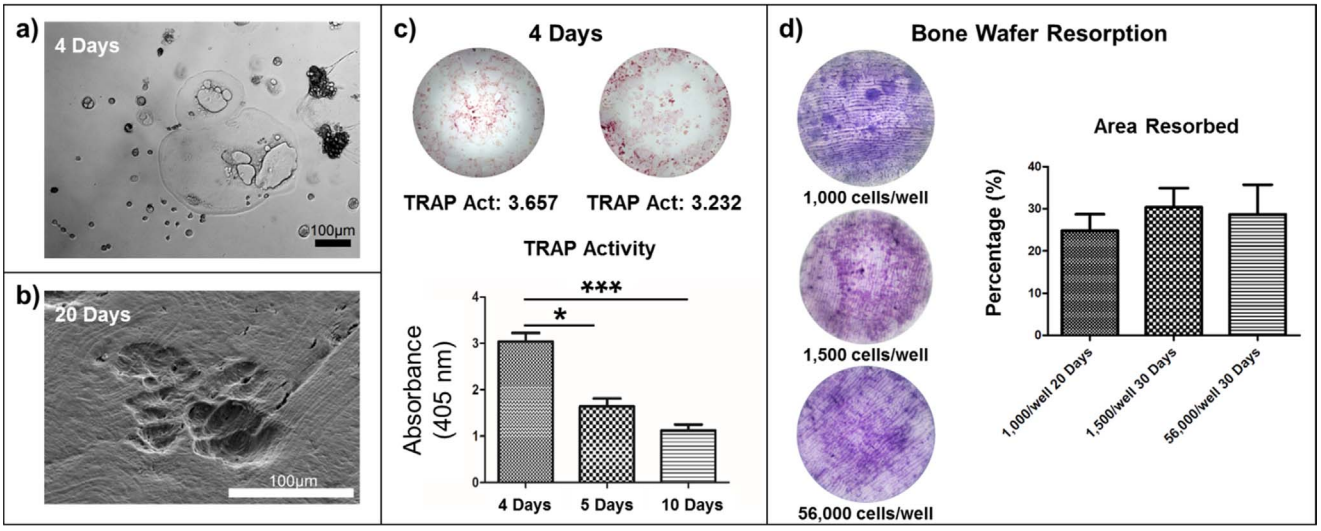

Fig. 10. Osteoclast Characterization. a) Phase image of RAW 264.7 cell 4 days post-induction on TC treated plate. b) SEM image of osteoclastic resorption on surface of bone wafer at 20 days (cells seeded at 1000 cells/well). c) Typical TRAP stains on TC treated polystyrene with activity quantification. d) Typical bone wafers showing pit staining at 20 days within 96-well plates and at 30 days of culture in LOC. Average resorption as determined by toluidine blue surface area staining was 24.9%, 30.4% and 28.7% for cells seeded at 1000 cells/well and cultured for 20 days, 1500 cells/well and cultured for 30 days and 56,000 cells/well and cultured for 30 days, respectively. Bone wafers measure approximately 6 mm in diameter. Error bars represent standard errors of the means.

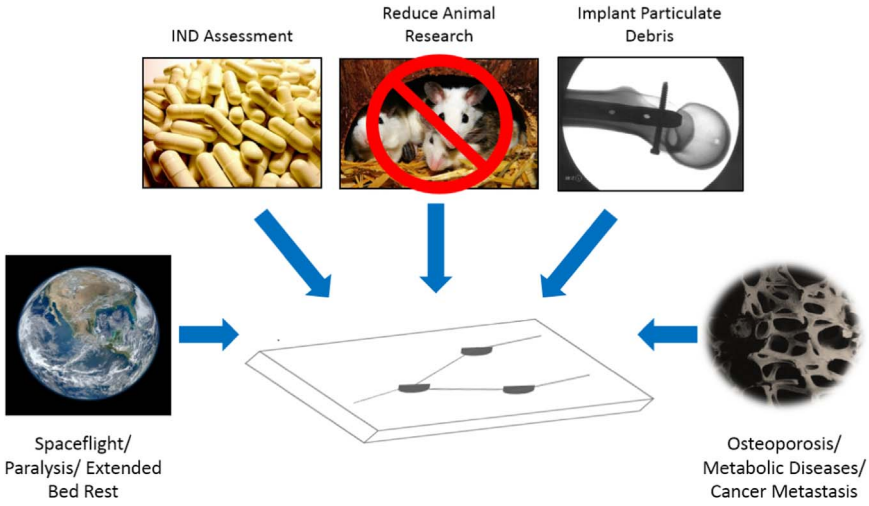

Fig. 11. Graphic depicting the potential of a remodeling LOC to facilitate exploration in the bone field.

subjected osteocytes to a brief bout of mechanical stimulation (15 min) at normal and elevated mechanical levels. Soluble factors were then assessed for their effects on bone formation. Supporting data have been included to demonstrate use of these LOCs under a sampling of environmental conditions. The goal is not to demonstrate that each treatment has a statistically significant effect, but that the effects are quantifiable. We believe that it is the totality of the multicellular interactions that needs to be modeled and will provide critical insights into remodeling. These interactions have yet to be incorporated into complex in vitro models—this is the immediate focus of our work. Whereas typical mechanotransduction research incorporates cell stimulation and marker activity, it is completed in isolation of the other cell types. The effects of differential activity on the other cell types and the expression of initial markers are not represented. Ultimately, these interactions provide a feedback system that is critical to incorporate in bone remodeling systems.

We plan to use our platforms to study certain pathologic conditions, such as fracture and osteonecrosis of the jaw. More specifically, we are interested in the effects of excessive mechanical load and bone deformation on bone cell mechanotransduction and functional activity. It is for this reason we have chosen to develop a mechanically loadable LOC with the capacity to reproducibly deform our PDMS substrates. It is worthy to note that out-of-plane distention is a complex load that integrates a primary distention load and a secondary fluid shear given that cells are submersed in medium. Importantly, strains applied to whole bone result in considerably greater microscopic strains around the osteocyte lacunae [26,36]. In fact, Nicolella et al. state that perilacunar strains may be more than an order of magnitude greater than the strains experienced by the bone tissue at the macroscopic level [26]. Because high tissue strain magnitudes of $\geq 5\%$ are implicated in pathologic bone conditions [43], we've enabled our platform to deform substrates to much higher levels. To that end, we have begun design of an automated multilayer LOC with the ability to cyclically shear osteocytes and deliver resulting soluble factors to osteoblasts and osteoclasts within the same device. In this way, we plan to study bone remodeling-related disorders associated with fluid flow-induced shear stress.

Given that fabrication techniques and proof of concept have been established, we are currently working to enhance physiological relevance and ease of use. For example, osteoblasts condition their environment and respond to autocrine/paracrine signals. Parallel experiments with MC3T3-E1 cells cultured on TC treated plates and within unlidded LOCs incorporated 50% media replacements during feedings. These cells formed significantly more bone than did cells within lidded LOCs. As such, modifications to the LOC design will be made to allow for 50% media replacements in future work. Additionally, automated feedings by use of pumps will minimize human involvement and enhance reproducibility. Side channels will be incorporated for appropriate cell seeding and to prevent cells from growing within main channels. Valves will be implemented to allow the flow of CM among wells and transmission of signals only when cells have been cultured and treated/induced for sufficient lengths of time. Upcoming work will incorporate co-cultures currently being established in our lab for bidirectional signaling, inhibited GJIC in osteoblast in addition to osteocyte networks and 3D osteocyte matrices for increased physiological relevance. In these ways, the redesign of our platforms will enhance both ease of use and reproducibility and strengthen biological validity.

Bone remodeling is an elegantly orchestrated process between bone cells. While much is currently known about the basic functions of the individual cell types, there is still much to understand of the process as a whole. For instance, with the help of macrophage-colony stimulating factor (MCSF-1) and RANKL, osteoclasts are able to adhere to the bone surface and resorb bone by creating an acidic microenvironment underneath the cell surface delineated from the extracellular environment via a sealing zone. Following the cessation of bone resorption, the bone formation phase ensues. The period between the cessation of osteoclast resorption and the initiation of osteoblast formation is known as the reversal phase—little is understood about this process. Currently, the reversal phase is assumed to last on the order of five weeks. That is, on average, there are five weeks between the time the last osteoclast leaves the bone surface and the first osteoblast appears [33]. As such, there is speculation as to what draws the osteoblasts to the surface and signals bone formation. Factors that have been implicated in this process include those secreted by the osteoclast—membrane-bound and matrix-derived factors. However, given the time involved, these factors, at most, are expected to act on osteoblast precursors. The remodeling canopy, previously discussed in Fig. 1, has been proposed as a possible physical barrier to isolate and retain the necessary coupling factors during the reversal phase. And, the osteocyte may do more than initiate remodeling, playing a key role in directing subsequent bone formation. Issues exist with these speculations. For example, ephrin is a membrane-bone factor proposed to mediate communication and coupling between osteoclasts and osteoblasts in a contact-dependent manner. Given that these cells are not on the bone surface at the same time, ephrin relevance has been called into question. However, research has suggested ephrin/eph binding from osteoclasts (ephrin) to osteoblasts (eph) drives new bone formation, while eph/ephrin binding from osteoblasts (eph) to osteoclasts (ephrin) ceases bone resorption simultaneously. However, the idea of bidirectional signaling is still in its

infancy. Further, the concept of canopy formation, while attractive, has not been observed in murine models, where much study of bone turnover takes place.

Cutting edge research is leading to the development of organs-on-a-chip, or organoids, that integrate microfluidic components on a single platform to recapitulate in vivo function. This effort has led to organ modeling of lung, kidney, blood and cancer, to name a few [22]. Augmentation of these systems is theoretically feasible, resulting in the human-on-a-chip model. However, bone is conspicuously absent from this work—we believe this is an oversight that needs corrected. A remodeling LOC that accurately recapitulates the in vivo function of bone offers tremendous opportunities for discovery and use in the bone field. These discoveries could apply to conditions and diseases, such as fracture healing, distraction osteogenesis, osteoporosis, osteopetrosis, bone metastasis, osteolysis and osteonecrosis of the joints. The introduction of implant debris into the system could enable the systematic study of particulate material, size and shape on bone cell activity in isolation and combination. Use of the chip in microgravity could provide a powerful model to systematically study the effects of weightlessness and unloading on bone. Earth-based studies could be completed on individual cell types using a Synthecon bioreactor, while use of the chip on the International Space Station could provide the combined interactions in microgravity. And, use of the platform in space could reduce payload by lessening and possibly eliminating the need for animal models. Commercialization could lead to a point-of-care device to test osteoporosis drug efficacy and investigational new drugs (INDs) for quantifying unintended side effects on bone activity (Fig. 11). In conclusion, work that may be carried out in this platform is compulsory to advancing the technology and exploiting avenues for potential discoveries in the bone field.

Acknowledgements

The authors would like to thank Miss Alexandria Magyar for assistance quantifying bone resorption.

Funding

This work was supported by the National Science Foundation [CBET 1060990 and EBMS 1700299] and the National Institutes of Health NIDCR [DE022664].

References

[1] M. Askmyr, K.E. White, T. Jovic, H.A. King, J.M. Quach, A.C. Maluenda, E.K. Baker, M.F. Smeets, C.R. Walkley, L.E. Purton, Ciliary neurotrophic factor has intrinsic and extrinsic roles in regulating B cell differentiation and bone structure, Sci. Rep. 5 (2015) 15529.
[2] Y. Bae, E. Oh, H.Y. Lee, H.J. Kim, Y.J. Park, Inhibitory effect of serum amyloid A on receptor activation of nuclear factor κB ligand-induced osteoclast formation (CAM1P.160), J. Immunol. 194 (1 Supplement) (2015) (48.17).
[3] K.A. Bhatt, E.I. Chang, S.M. Warren, S.E. Lin, N. Bastidas, S. Ghali, A. Thibboneir, J.M. Capla, J.G. McCarthy, G.C. Gurtner, Uniaxial mechanical strain: an in-vitro correlate to distraction osteogenesis, J. Surg. Res. 143 (2) (2007) 329–336.
[4] G.N. Brown, R.L. Sattler, X.E. Guo, Experimental studies of bone mechanoadaptation: bridging in vitro and in vivo studies with multiscale systems, Interface Focus 6 (1) (2016) 20150071.
[5] J.C. Chen, M. Chua, R.B. Bellon, C.R. Jacobs, Epigenetic changes during mechanically induced osteogenic lineage commitment, J. Biomech. Eng. 137 (2) (2015) 020902.
[6] B. Cheng, Y. Kato, S. Zhao, J. Luo, E. Sprague, L.F. Bonewald, J.X. Jiang, PGE2 is essential for gap junction-mediated intercellular communication between osteocyte-like MLO-Y4 cells in response to mechanical strain, Endocrinology 142 (8) (2001) 3464–3473.
[7] C.T. Culbertson, T.G. Mickleburgh, S.A. Stewart-James, K.A. Sellens, M. Pressnall, Micro total analysis systems: fundamental advances and biological applications, Anal. Chem. 86 (1) (2014) 95–118.
[8] J. Delaisse, The reversal phase of the bone-remodeling cycle: cellular prerequisites for coupling resorption and formation, BoneKey Rep. 3 (2014) 561.
[9] J. El-Ali, P.K. Sorger, K.F. Jensen, Cells on chips, Nature 442 (2006) 403–411.
[10] S.A. Ely, D.M. Knowles, Expression of CD56/neural cell adhesion molecule correlates with the presence of lytic bone lesions in multiple myeloma and distinguishes myeloma from monoclonal gammopathy of undetermined significance and lymphomas with plasmacytoid differentiation, Am. J. Pathol. 160 (4) (2002) 1293–1299.
[11] E.W. Esch, A. Bahinski, D. Huh, Organs-on-chips at the frontiers of drug discovery, Nat. Rev. Drug Discov. 14 (4) (2015) 248–260.
[12] A.M. Ghaemmaghami, M.J. Hancock, H. Harrington, H. Kaji, A. Khademhosseini, Biomimetic tissues on a chip for drug discovery, Drug Discov. Today 17 (3–4) (2012) 173–181.
[13] P.M. Govey, J.M. Jacobs, S.C. Tilton, A.E. Loiselle, Y. Zhang, W.M. Freeman, K.M. Waters, N.J. Karin, H.J. Donahue, Integrative transcriptomic and proteomic analysis of osteocytic cells exposed to fluid flow reveals novel mechano-sensitive signaling pathways, J. Biomech. 47 (8) (2014) 1838–1845.
[14] J.R. Hens, K.M. Wilson, P. Dann, X. Chen, M.C. Horowitz, J.J. Wysolmerski, TOPGAL mice show that the canonical Wnt signaling pathway is active during bone development and growth and is activated by mechanical loading in vitro, J. Bone Miner. Res. 20 (7) (2005) 1103–1113.
[15] C.T. Hung, F.D. Allen, S.R. Pollack, C.T. Brighton, Intracellular Ca2+ stores and extracellular Ca2+ are required in the real-time Ca2+ response of bone cells experiencing fluid flow, J. Biomech. 29 (11) (1996) 1411–1417.
[16] W. Katagiri, M. Osugi, T. Kawai, H. Hibi, Secreted frizzled-related protein promotes bone regeneration by human bone marrow-derived mesenchymal stem cells, Int. J. Mol. Sci. 16 (10) (2015) 23250–23258.
[17] J.D. King, D. Hayes, K.S. Shah, S.L. York, P. Sethu, M.M. Saunders, Development of a multi-strain profile for cellular mechanotransduction testing, in: F. Barthelat, C. Korach, P. Zavattieri, B.C. Prorok, K.J. Grande-Allen (Eds.), Mechanics of Biological Systems and Materials, vol. 7: Proceedings of the 2014 Annual Conference on Experimental and Applied Mechanics, Springer, New York, 2014, pp. 61–67.
[18] J. Klein-Nulend, A. van der Plas, C.M. Semeins, N.E. Ajubi, J.A. Frangos, P.J. Nijweide, E.H. Burger, Sensitivity of osteocytes to biomechanical stress in vitro, FASEB J. 9 (5) (1995) 441–445.
[19] S.J. Lee, S.Y. Lee, Micro total analysis system (μ-TAS) in biotechnology, Appl. Microbiol. Biotechnol. 64 (3) (2004) 289–299.
[20] L. Liu, C. Li, X. Cai, J. Xiang, Z. Cao, W. Dong, The temporal expression and localization of extracellular matrix metalloproteinase inducer (EMMPRIN) during the development of periodontitis in an animal model, J. Periodontal Res. 45 (4) (2010) 541–549.
[21] S.C. Manolagas, Birth and death of bone cells: basic regulatory mechanisms and implications for the pathogenesis and treatment of osteoporosis, Endocr. Rev. 21 (2) (2000) 115–137.
[22] V. Marx, Tissue engineering: organs from the lab, Nature 522 (7556) (2015) 373–377.
[23] K. Middleton, S. Al-Dujaili, X. Mei, A. Günther, L. You, Microfluidic co-culture platform for investigating osteocyte-osteoclast signalling during fluid shear stress mechanostimulation, J. Biomech. 59 (2017) 35–42.
[24] C. Moraes, G. Mehta, S.C. Lesher-Perez, S. Takayama, Organs-on-a-chip: a focus on compartmentalized microdevices, Ann. Biomed. Eng. 40 (2012) 1211–1227.
[25] P.J. Neame, C.J. Kay, D.J. McQuilan, M.P. Beales, J.R. Hassell, Independent modulation of collagen fibrillogenesis by decorin and lumican, Cell. Mol. Life Sci. 57 (5) (2000) 859–863.
[26] D.P. Nicolella, D.E. Moravits, A.M. Gale, L.F. Bonewald, J. Lankford, Osteocyte lacunae tissue strain in cortical bone, J. Biomech. 39 (9) (2006) 1735–1743.
[27] A.G. Robling, C.H. Turner, Mechanical signaling for bone modeling and remodeling, Crit. Rev. Eukaryot. Gene Expr. 19 (4) (2009) 319–338.
[28] M.M. Saunders, Biomimetics in bone cell mechanotransduction: understanding bone's response to mechanical loading, in: A. George (Ed.), Adv. Biomimetics, InTech, Rijeka, 2011, pp. 317–348.
[29] M.M. Saunders, A.F. Taylor, C. Du, Z. Zhou, V.D. Pellegrini, H.J. Donahue, Mechanical stimulation effects on functional end effectors in osteoblastic MG-63 cells, J. Biomech. 39 (8) (2006) 1419–1427.
[30] M.M. Saunders, J. You, Z. Zhou, Z. Li, C.E. Yellowley, E. Kunze, C.R. Jacobs, H.J. Donahue, Fluid flow-induced prostaglandin E2 response of osteoblastic ROS 17/2.8 cells is gap junction-mediated and independent of cytosolic calcium, Bone 32 (4) (2003) 350–356.
[31] A. Scott, K.M. Khan, V. Duronio, D.A. Hart, Mechanotransduction in human bone: in vitro cellular physiology that underpins bone changes with exercise, Sports Med. 38 (2) (2008) 139–160.
[32] K. Shah, S. York, P. Sethu, M.M. Saunders, Developing a microloading platform for applications in mechanotransduction research, in: B.C. Prorok, F. Barthelat, C.S. Korach, K.J. Grande-Allen, E. Lipke (Eds.), Mechanics of Biological Systems and Materials, vol. 5: Proceedings of the 2012 Annual Conference on Experimental and Applied Mechanics, Springer, New York, 2012, pp. 197–205.
[33] N.A. Sims, T.J. Martin, Coupling signals between the osteoclast and osteoblast: how are messages transmitted between these temporary visitors to the bone surface? Front. Neuroendocrinol. 6 (2015) 41.
[34] N.A. Sims, T.J. Martin, Coupling the activities of bone formation and resorption: a multitude of signals within the basic multicellular unit, BoneKEy Rep. 3 (2014) 481.
[35] M. Swanberg, F. McGuigan, K.K. Ivaska, P. Gerdhem, U.H. Lerner, R. Bucala, G. Kuchel, A. Kenny, K. Åkesson, Polymorphisms in the macrophage migration inhibitory factor gene and bone loss in postmenopausal women, Bone 47 (2) (2010) 424–429.
[36] T. Takano-Yamamoto, Osteocyte function under compressive mechanical force, Jpn. Dent. Sci. Rev. 50 (2) (2014) 29–39.
[37] M. Tzaphlidou, Bone architecture: collagen structure and calcium/phosphorus maps, J. Biol. Phys. 34 (1–2) (2008) 39–49.
[38] S.L. York, A.R. Arida, K.S. Shah, M.M. Saunders, Osteocyte characterization on

polydimethylsiloxane substrates for microsystems applications, J. Biomim. Biomater., Tissue Eng. 16 (1) (2012) 27–42.
[39] S.L. York, J.D. King, A.S. Pietros, B. Zhang Newby, P. Sethu, M.M. Saunders, Development of a microloading platform for in vitro mechanotransduction studies, in: F. Barthelat, C. Korach, P. Zavattieri, B.C. Prorok, K.J. Grande-Allen (Eds.), Mechanics of Biological Systems and Materials, vol. 7: Proceedings of the 2014 Annual Conference on Experimental and Applied Mechanics, Springer, New York, 2014, pp. 53–69.
[40] S.L. York, P. Sethu, M.M. Saunders, Impact of mechanical load and gap junctional intercellular communication on MLO-Y4 sclerostin and soluble factor expression, Ann. Biomed. Eng. 44 (2015) 1170.
[41] S.L. York, P. Sethu, M.M. Saunders, In vitro osteocytic microdamage and viability quantification using a microloading platform, Med Eng. Phys. 38 (2016) 1115–1122.
[42] S.L. York, K.S. Shah, M.M. Saunders, Biomimicry, microsystems and bone, in: A. Scipione (Ed.), Focus on Biomimetics Research, Nova Science Publishers, 2013, pp. 1–42.
[43] J. You, C.E. Yellowley, H.J. Donahue, Y. Zhang, Q. Chen, C.R. Jacobs, Substrate deformation levels associated with routine physical activity are less stimulatory to bone cells relative to loading-induced oscillatory fluid flow, J. Biomech. Eng. 122 (4) (2000) 387–393.